Published in final edited form as:
Biochim Biophys Acta. 2012 July ; 1822(7): 1169–1179. doi:10.1016/j.bbadis.2011.10.007.

Increased cone sensitivity to ABCA4 deficiency provides insight into macular vision loss in Stargardt's dystrophy

Shannon M. Conley[a,1], **Xue Cai**[a,1], **Rasha Makkia**[a], **Yalin Wu**[b], **Janet R. Sparrow**[b], and **Muna I. Naash**[a,*]

[a]University of Oklahoma Health Sciences Center, Department of Cell Biology, Oklahoma City, OK, USA

[b]Departments of Ophthalmology and Pathology & Cell Biology, Columbia University, New York City, NY, USA

Abstract

Autosomal recessive Stargardt macular dystrophy is caused by mutations in the photoreceptor disc rim protein ABCA4/ABCR. Key clinical features of Stargardt disease include relatively mild rod defects such as delayed dark adaptation, coupled with severe cone defects reflected in macular atrophy and central vision loss. In spite of this clinical divergence, there has been no biochemical study of the effects of ABCA4 deficiency on cones vs. rods. Here we utilize the cone-dominant $Abca4^{-/-}/Nrl^{-/-}$ double knockout mouse to study this issue. We show that as early as post-natal day (P) 30, $Abca4^{-/-}/Nrl^{-/-}$ retinas have significantly fewer rosettes than $Abca4^{+/+}/Nrl^{-/-}$ retinas, a phenotype often associated with accelerated degeneration. *Abca4*-deficient mice in both the wild-type and cone-dominant background accumulate more of the toxic bisretinoid A2E than their ABCA4-competent counterparts, but $Abca4^{-/-}/Nrl^{-/-}$ eyes generate significantly more A2E per mole of 11-*cis*-retinal (11-cisRAL) than $Abca4^{-/-}$ eyes. At P120, $Abca4^{-/-}/Nrl^{-/-}$ produced 340±121 pmoles A2E/nmol 11-cisRAL while $Abca4^{-/-}$ produced 50.4±8.05 pmoles A2E/nmol 11-cisRAL. Nevertheless, the retinal pigment epithelium (RPE) of $Abca4^{-/-}/Nrl^{-/-}$ eyes exhibits fewer lipofuscin granules than the RPE of $Abca4^{-/-}$ eyes; at P120: $Abca4^{-/-}/Nrl^{-/-}$ exhibit 0.045±0.013 lipofuscin granules/μm^2 of RPE vs. $Abca4^{-/-}$ 0.17±0.030 lipofuscin granules/μm^2 of RPE. These data indicate that ABCA4-deficient cones simultaneously generate more A2E than rods and are less able to effectively clear it, and suggest that primary cone toxicity may contribute to Stargardt's-associated macular vision loss in addition to cone death secondary to RPE atrophy.

Keywords

ABCA4; Cone; Retinal degeneration; Stargardt's; A2E

1. Introduction

ABCA4, a retina-specific member of the ATP-binding cassette transporter family, (formerly known as ABCR or rim protein/RmP), is a 220 kD member of the ATP-binding cassette (ABC) family of protein transporters [1–3]. Mutations and polymorphisms in ABCA4 are associated primarily with recessive Stargardt macular dystrophy but also with age-related macular degeneration, retinitis pigmentosa, and a form of cone-rod dystrophy [4]

*Corresponding author at: OUHSC, Department of Cell Biology, 940 Stanton L. Young Blvd. BMSB 781, Oklahoma City, OK 73104, USA. Tel.: +1 405 271 2388; fax: +1 405 271 3548. muna-naash@ouhsc.edu (M.I. Naash).
[1]These two authors contributed equally to this work.

(http://www.retina-international.org/sci-news/abcrmut.htm). Stargardt's is characterized by delayed dark adaptation, significant accumulation of lipofuscin in the retinal pigment epithelium (RPE), fundus flecks, macular atrophy, and subsequent loss of central vision [1,2].

ABCA4 is localized to the disc rims of photoreceptor outer segments (OSs) [2,5] and most likely functions as a flippase for retinoids released from opsin after excitation by light [6]. In the dark, both rod and cone opsins are bound to 11-*cis*-retinal (11-cisRAL) which is rapidly isomerized to all-*trans*-retinal (atRAL) upon illumination. atRAL is then released from the opsin protein and is recycled into 11-cisRAL in the visual cycle. The first metabolic step in the visual cycle is the reduction of atRAL to all-*trans*-retinol in the OS cytosol. ABCA4 is thought to be responsible for transporting a portion of atRAL from the lumen to the cytoplasmic side of the membrane to facilitate retinoid recycling [7]. Although membrane transport assays for ABCA4 are not available, ATPase activity assays have indicated that the preferred substrate for ABCA4 is the Schiff base adduct of atRAL and phosphatidylethanolamine (PE) [8]. Normally these compounds are recycled back into 11-cisRAL, but they can form permanent di-retinal species such as the pyridinium bis-retinoid A2E and its isomers iso-A2E and precursor A2PE [9,10]. Although these compounds do accumulate in the normal eye, in certain disease states they accumulate much more rapidly. As the photoreceptor OSs are phagocytosed by the RPE, A2E and related bisretinoids accumulate in RPE lysosomes as autofluorescent material called lipofuscin. There are several ways A2E is thought to cause RPE toxicity, including destabilizing membranes [11,12], generating reactive oxygen species, and photooxidation [13,14]. A2E and its oxidation products have also been shown to activate complement by the alternative pathway [15], a system often dysregulated in age-related macular degeneration.

Stargardt maculopathy is the best characterized of the ABCA4-associated diseases and significant research has gone into the mechanism underlying it. The clinical signs and symptoms of Stargardt's can be easily explained biochemically. Interestingly, these symptoms seem to target rods and cones differently. One of the key disease features is delayed dark adaptation- a rod-related phenotype generally assumed to result from re-formation of a non-functional atRAL–opsin complex when atRAL is not efficiently cleared by ABCA4. In contrast, the severest loss of vision is associated with the cone-dominant macula. This abnormality is generally attributed not to direct cone defects but to atrophy of RPE cells in the macula as a result of A2E bisretinoid accumulation with subsequent degeneration of cone cells.

Genetically engineered *Abca4* knockout mice ($Abca4^{-/-}$) exhibit some disease symptoms similar to Stargardt's patients; namely delayed dark adaptation, enhanced retinal autofluorescence and increased accumulation of A2E [2,16]. The fundus of aged $Abca4^{-/-}$ mice also exhibits disease markers, specifically whitish-yellow flecks and the appearance of atrophic, degenerated areas (Fig. 1 arrows). Unfortunately, the mouse does not have a macula; and indeed the mouse retina contains only about 3–5% cones. Thus biochemical studies that provide insight into the way rods use ABCA4 and process retinoids provide little information as to cones and can furnish little information on the actual pathobiology underlying cone and macular vision loss. To help address this deficit, we take advantage of the $Nrl^{-/-}$ mouse model [17,18]. In the absence of the Nrl transcription factor, rods are converted to cone-like photoreceptors which express cone proteins and exhibit cone electrophysiological and structural features. Although the cones of the $Nrl^{-/-}$ are not identical to wild-type murine cones, the advantages provided by this model cannot be mimicked by any other murine model and provide us an unparalleled opportunity to study the effects of ABCA4 deficiency on cones. The $Nrl^{-/-}$ retina exhibits two key features which mimic the human macula: 1) cones are expressed densely and cone OSs abut one another

without interpolation of rods, and 2) cone OSs are adjacent to the RPE (except those inside rosettes) instead of being obscured by rods. By generating the *Abca4*$^{-/-}$/*Nrl*$^{-/-}$ double knockout mouse we have shown that cones are more affected than rods by ABCA4 deficiency and provide insight into why ABCA4 deficiency can cause a relatively minor rod defect (delayed dark adaptation) and a severe cone defect (loss of central vision).

2. Materials and methods

2.1. Animal care and use

Pigmented *Abca4*$^{-/-}$/*Nrl*$^{-/-}$ mice homozygous for the leucine 450 RPE65 variant were generated from *Nrl*$^{-/-}$ (generously shared by Dr. Anand Swaroop, NEI) and *Abca4*$^{-/-}$ (generously shared by Dr. Gabriel Travis, Jules Stein Eye Institute) single knockouts. Adult mice (WT-*Abca4*$^{+/+}$/*Nrl*$^{+/+}$, *Abca4*$^{-/-}$/*Nrl*$^{+/+}$, *Abca4*$^{+/+}$/*Nrl*$^{-/-}$, and *Abca4*$^{-/-}$/*Nrl*$^{-/-}$) were reared in a 12-hour light–dark cycle with an ambient light intensity of 30 lx. Some cohorts were transferred at post-natal day (P) 5 to a light box (12 h light–dark cycle, ambient light 300 lx) where they were reared thereafter. All animal protocols used in these experiments were approved by the local Institutional Animal Care and Use Committee (Oklahoma City, OK, USA) and were in accordance with the guidelines on the care and use of animals in research as established by the Society for Neuroscience and the Association for Research in Vision and Ophthalmology.

2.2. Fundus imaging

Fundus imaging was conducted using the Micron III imaging system with mouse objective from Phoenix Research Labs (Pleasanton, CA). Animals were anesthetized by intramuscular injection of 85 mg/kg ketamine and 14 mg/kg xylazine (Pharmaceutical Systems, Inc., Tulsa, OK). Eyes were dilated with 1% Cyclogyl (Alcon, USA), and a drop of 2.5% methylcellulose (Pharmaceutical Systems Inc.) was placed on the corneal surface. Mice were placed on an adjustable stage and the Micron III objective was stereoscopically adjusted until it came into contact with the cornea. Images were then captured using the StreamPix software (Phoenix Research Labs).

2.3. Light and electron microscopy

Eyes were collected from 3 to 5 dark-adapted animals per group. The superior cornea was marked prior to enucleation and samples were dissected, fixed, embedded, and sectioned as described previously [19,20]. Semithin sections were stained with 1% toluidine blue in 1% sodium borate and imaged with an Olympus BH-2 microscope. Ultrathin sections were stained with 2% uranyl acetate and lead citrate and imaged using a JEOL 100CX electron microscope (Japan).

2.4. Morphometry

For light morphometry, semithin sections along the nasal/temporal axis were imaged under a 40× objective at increasing distances from the optic nerve head. The number of cells in a 220 μm section (the width of a 40× image) of the outer nuclear layer in each image was counted. To quantify rosette number, images were captured and the number of rosettes was counted across an entire central retinal section (containing the optic nerve head). Images from 3 to 5 animals per group were analyzed. Data are presented as means±SEM. For electron microscopy (EM) morphometry, ultrathin sections along the nasal/temporal plane were imaged at 6000×. Lipofuscin granules and phagocytosed OSs were counted manually and Adobe Photoshop CS3 was used to determine RPE area and the size of lipofuscin granules. At least 5 images per eye were evaluated and to account for variations in the amount of RPE visible in each image, results from each of the 5 images were summed to give individual values for each eye, and values are normalized to the area of the RPE.

Analyses were done on 3–6 animals per genotype (all at P120) and results are analyzed by two-way ANOVA with Bonferroni's post-hoc test.

2.5. Immunofluorescence labeling

Eyes were collected and fixed as described above and were then embedded and cryosectioned as described previously [21]. Immunofluorescence labeling was performed as described previously using monoclonal antibody MAB360 (Chemicon International, Temecula, CA) against glial fibrillary acid protein (GFAP). Slides were imaged on an Olympus BX-62 microscope equipped with a spinning disc confocal unit. Images were stored and deconvolved (no neighbors paradigm) using Slidebook® version 4.2 and are single slices of a confocal stack.

2.6. Electroretinography

Full field scotopic and photopic ERG was performed on anesthetized mice at P30, P60 and P120 after overnight dark-adaption using the UTAS system (LKC, Gaithersburg, MD, USA) as described previously [20,21]. Scotopic responses were measured after a single strobe flash at 157 cd s/m^2. Animals were then light adapted for 5 min (29.03 cd/m^2) and photopic responses were measured by averaging 25 flashes at 79 cd s/m^2. At least 5–10 animals were examined per age, light intensity, and genotype. Data are presented as means ±SEM. Two-way ANOVA and Bonferroni's post-hoc test were used to determine statistical significance.

2.7. Analysis of A2E, other bis-retinoids, and 11-cisRAL

Animals were dark-adapted overnight, and eyecups were collected in the dark and immediately frozen in liquid nitrogen. The eyecups were homogenized, extracted, filtered, and evaporated. The extract was re-dissolved in methanol/chloroform and A2E and iso-A2E were measured using HPLC (Alliance system, Waters, Corp, Milford, MA) as previously described [22]. Four eyes were combined for each A2E measurement. 11-cisRAL measurements were conducted under dim red light. Mouse eyecups were homogenized in methanol/50% hydroxyl-amine aqueous solution, incubated for 30 min, and extracted three times with chloroform. The organic phases were collected and dried under argon. The dried samples were redissolved in 80 μl methanol and 40 μl was injected into HPLC (Waters 2695). Chromatography was performed using a normal phase column (Agilent ZORBAX Rx-SIL; 4.6×250 mm, 5 μm) and elution with a gradient of hexane (A) and 1,4-dioxane (B): 0–45 min, 100-95% A, 1.5 ml/min; 45–60 min, 95-90% A, 1.5 ml/min; 60–70 min, 90% A, 1.5 ml/min. Absorbance peaks were identified by comparison with external standards (11-cisRAL was a kind gift from Dr. Rosalie Crouch to Dr. Janet Sparrow), and molar quantities per eye were calculated by comparison to standard concentrations determined spectrophotometrically using published extinction coefficients, and normalized to total sample volumes. Statistical analysis was performed using two way ANOVA (light and genotype) while 11-cisRAL results were analyzed by one-way ANOVA (genotype), both using Bonferroni's post-hoc test.

3. Results

3.1. Structural effects of ABCA4 deficiency in cones

It has been shown that retinal degeneration in the *Abca4*$^{-/-}$ mouse does not begin until around the 8th month of life [23]. To determine whether degeneration is more rapid in *Abca4*$^{-/-}$/*Nrl*$^{-/-}$ or in animals raised in bright light (300 lx), tissues were collected at P30, 60, and 120 from animals reared in both dim (30 lx) and bright light. Representative light microscopic images are shown in Fig. 2A for WT (*Abca4*$^{+/+}$/*Nrl*$^{+/+}$) and *Abca4*$^{-/-}$ (*Abca4*$^{-/-}$/*Nrl*$^{+/+}$) and in Fig. 2B for *Nrl*$^{-/-}$ (*Abca4*$^{+/+}$/*Nrl*$^{-/-}$) and *Abca4*$^{-/-}$/*Nrl*$^{-/-}$. No overt alterations in retinal structure are observed in *Abca4*$^{-/-}$ eyes at any age when compared to

WT. *Nrl*$^{-/-}$ animals exhibit characteristic whorls [18] in the outer nuclear layer (ONL) called rosettes. As shown in Fig. 2B–C, *Abca4*$^{-/-}$/*Nrl*$^{-/-}$ animals exhibit significantly fewer rosettes than *Nrl*$^{-/-}$ animals at all ages. The reduction in rosettes does not appear to be age dependent; the number of rosettes observed in *Abca4*$^{-/-}$/*Nrl*$^{-/-}$ animals is not significantly different at P30, 60, or 120. As the overall number of rosettes in *Nrl*$^{-/-}$ animals decreases slightly with age, the difference in rosette number between *Abca4*$^{-/-}$/*Nrl*$^{-/-}$ and *Nrl*$^{-/-}$ animals is most pronounced at P30. Rearing animals in bright light does not appear to have a significant effect on retinal structure or rosette number.

The *Nrl*$^{-/-}$ retina degenerates over time [24,25], and to determine whether this degeneration is accelerated by the absence of ABCA4, we counted the number of photoreceptor nuclei in a 220 μm section of the ONL at increasing intervals from the optic nerve head. In the WT (*Nrl*$^{+/+}$) background we observed no changes in the ONL at any time-point, age, or lighting condition (Fig. 3A). In the *Nrl*$^{-/-}$ background (Fig. 3B), we observed decreases in the number of cells in the ONL at P60 and P120 compared to P30 (gray line) but neither the absence of ABCA4 (*Abca4*$^{-/-}$/*Nrl*$^{-/-}$) nor exposure to light accelerates the rate of cone cell death.

In keeping with the lack of significant structural changes in mice lacking ABCA4, we observed no significant light or age-dependent ultrastructural changes in OSs of mice lacking ABCA4 in either the WT or *Nrl*$^{-/-}$ backgrounds (Supplementary Fig. 1).

To determine whether the development of the abnormal fundus phenotype shown in Fig. 1 was accelerated in the cone dominant background, fundus images were taken at 2–3 months and at 4–5 months of age from mice of all 4 genotypes. At both timepoints we examined, *Abca4*$^{-/-}$ eyes exhibited variability in fundus phenotype. At 2–3 months of age, half of the eyes examined (3/6) had a completely normal fundus phenotype while the fundi of other animals exhibited white spots (3/6). By 4–5 months, more eyes exhibited these white spots (4/5), but not all. None of the WT eyes exhibited these white spots at either age (0/6 at 2–3 months and 0/5 at 4–5 months). These spots may be early signs of retinal flecking (Fig. 4A, black arrows), but others have suggested that white spots may correlate with the appearance of microglia. The most striking feature of the *Nrl*$^{-/-}$ retina is the appearance of light gray spots all over the fundus (Fig. 4B, white arrows). These spots are in a different plane from other retinal features and likely correspond to rosettes. Support for this comes from fundus images of *rds*$^{-/-}$/*Nrl*$^{-/-}$ mice (a genotype which has significantly reduced rosettes [24]); they lack the gray spots (not shown). In keeping with this idea, we observe fewer gray-white spots in the *Abca4*$^{-/-}$/*Nrl*$^{-/-}$ mice than in the *Nrl*$^{-/-}$ at 2–-3 months and virtually no spots in double knockout animals at 4–-5 months. Similarly, fewer gray white spots are observed in the central retina of *Nrl*$^{-/-}$ animals at 4–5 months than at 2–3 months, consistent with the natural reduction in rosette number that occurs as degeneration begins in the *Nrl*$^{-/-}$ background. We observe that the fundi of animals in the *Nrl*$^{-/-}$ background are generally splotchier (i.e. more patchy variation in background color). We did not detect signs of retinal flecking in *Nrl*$^{-/-}$ or *Abca4*$^{-/-}$/*Nrl*$^{-/-}$ animals at either age, although the presence of rosettes and the patchier pattern of the fundi makes them difficult to analyze.

3.2. Retinal stress is detected in Abca4$^{-/-}$/Nrl$^{-/-}$ animals

Although we did not detect any significant ABCA4-associated degeneration in either the WT or *Nrl*$^{-/-}$ backgrounds (up to 4 months of age), we asked whether mice lacking ABCA4 exhibited any signs of increased retinal stress compared to controls. Immunofluorescent labeling with antibodies against glial fibrillary acid protein (GFAP), a retinal stress marker, indicated that GFAP was upregulated in retinas lacking ABCA4 (Fig. 5). In WT retinas, GFAP expression is limited to the Müller cell endfeet in the inner limiting membrane. In contrast, in *Abca4*$^{-/-}$ retinas, mild induction in GFAP is observed at P30, with patchy

extensions into the inner plexiform layer (IPL) at P60 (arrows). By P120, *Abca4*$^{-/-}$ eyes exhibit significant GFAP induction throughout the retina while the staining pattern in WT retinas remains normal. In contrast GFAP was induced in the *Nrl*$^{-/-}$ retina by P120 due to ongoing slow degeneration in this model. Induction of GFAP is accelerated in *Abca4*$^{-/-}$/*Nrl*$^{-/-}$ retinas compared to both single knockouts. Furthermore, staining in these double knockout retinas is more extensive than in any other genotype; at P120 GFAP labeling is detected through the IPL, inner nuclear layer (INL) and in some cases into the outer nuclear layer (ONL).

3.3. Cone function is not affected by the absence of ABCA4

It has been previously demonstrated that rod dark adaptation is delayed in *Abca4*$^{-/-}$ mice compared to wild-type mice [2,16], but that overall rod function is not affected. Since macular cone vision loss is a key phenotype of Stargardt's, we assessed whether cone function was affected in the absence of ABCA4. Full-field photopic ERGs were conducted at P30, 60 and 120 on animals raised at 30 lx and 300 lx. Consistent with our structural findings, light exposure had no effect on cone function. In the WT background, maximum photopic ERG responses were not different at any age or genotype (Fig. 6A). Maximum photopic ERG responses were reduced with significance in double knockout mice at P120 compared to P30 (22.8% reduction in animals raised at 300 lx, 21.3% reduction in animals raised at 30 lx—Fig. 6B), but no additional differences were detected. As this difference was not detected in cones in the WT background, it may be attributable to the onset of degeneration or the higher cone density of the *Nrl*$^{-/-}$ retina.

3.4. A2E levels are significantly increased in the absence of ABCA4

One of the primary defects in both human patients carrying *ABCA4* mutations and the *Abca4*$^{-/-}$ mouse is abnormal accumulation of A2E and other bisretinoids; this increase is also reflected in an increase in the RPE lysosomal organelles housing the lipofuscin (lipofuscin granules). The bisretinoid precursor of A2E, A2PE, is generated from atRAL within OS discs in the absence of the flippase activity of ABCA4 and then accumulates in the RPE as a result of phagocytosis of OSs. To determine whether abnormal amounts of A2E are generated in the cone-dominant retina, we harvested whole eyes from animals raised at 30 or 300 lx at P30, 60, and 120 and processed them for HPLC to measure total A2E levels (Fig. 7, chromatogram in Supplementary Fig. 2). Results were analyzed by two-way ANOVA (for light and genotype), and light was not a significant interacting variable at any age; genotype accounted for the observed variability. At P120, mean A2E levels in *Abca4*$^{-/-}$/*Nrl*$^{-/-}$ animals raised at 300 lx were less than in animals raised at 30 lx, but this difference was not significant. A2E levels increased with age, as expected, but at no age were differences detected between WT and *Nrl*$^{-/-}$ animals. In contrast, in the absence of ABCA4, A2E levels were significantly higher at every age and background. The difference is most pronounced at P120; A2E levels in *Abca4*$^{-/-}$ and *Abca4*$^{-/-}$/*Nrl*$^{-/-}$ are significantly higher than WT and *Nrl*$^{-/-}$. Although absolute accumulation in *Abca4*$^{-/-}$/*Nrl*$^{-/-}$ was less than in *Abca4*$^{-/-}$, the relative increase compared to controls was similar: A2E levels at P120 in *Abca4*$^{-/-}$ eyes were 3.17 and 3.76 fold higher than in WT animals (30/300 lx) while A2E levels in *Abca4*$^{-/-}$/*Nrl*$^{-/-}$ eyes were 3.08 and 2.08 fold higher than in *Nrl*$^{-/-}$.

Although the number of photoreceptor cells in the *Nrl*$^{-/-}$ retina is the same as the WT, structural data indicate that there is significantly less mass of OSs as a result of the lack of rods and the fact that *Nrl*$^{-/-}$ cones are shorter than WT cones. This decrease in OS mass is accompanied by an expected decrease in 11-cisRAL levels [26]. To take this into account we therefore measured 11-cisRAL levels in whole eyes at P120 (Fig. 8a), and since light had not been a significant variable in previous experiments, this experiment was conducted in animals reared at 30 lx. Levels were modestly reduced in the absence of ABCA4: levels in

Abca4$^{-/-}$ were reduced by an average of 30.4% compared to WT levels and levels in *Abca4*$^{-/-}$/*Nrl*$^{-/-}$ were reduced by an average of 50.8% compared to *Nrl*$^{-/-}$. The most striking difference, however, is that 11-cisRAL levels in *Nrl*$^{-/-}$ are reduced by 86.7% compared to WT, making levels in WT eyes almost 10 times higher than in *Nrl*$^{-/-}$ eyes. Since the starting material for generating A2E is the all-*trans*-retinal that forms when 11-cisRAL undergoes photoisomerization, it makes sense to express A2E levels as a function of 11-cisRAL. For clarity's sake we have re-plotted A2E levels at P120 in Fig. 8b (both light levels combined), and in Fig. 8C shows pmoles of A2E/eye as a function of pmoles of 11-cisRAL/eye. These results show that, per pmole of 11-cisRAL, abnormal A2E buildup in the absence of *Abca4*$^{-/-}$ is significantly higher in the cone-dominant background than in the rod-dominant background: levels of A2E/pmole of 11-cisRAL in double knockout eyes were 32.5 fold higher than in WT eyes, 6.8 fold higher than in *Abca4*$^{-/-}$ eyes and 5.9 fold higher than in *Nrl*$^{-/-}$ eyes.

3.5. Fewer RPE lipofuscin granules are detected in the cone-dominant background than in the rod-dominant background

Finally, we conducted ultrastructural morphometric analysis of RPE cell layers from eyes collected at P120 to determine whether A2E generated in cone OSs also contributes to the formation of lipofuscin granules in the RPE. For each eye, at least five images were analyzed and summed; we measured the total area of RPE in each image, the number and size of lipofuscin granules (black arrows—Fig. 9A), and the number of phagocytosed OS clumps (white arrows—Fig. 9A). As shown in Fig. 9B, the number of lipofuscin granules detected in the RPE of *Abca4*$^{-/-}$ eyes was significantly higher than the number in WT, and significantly higher than the number in *Abca4*$^{-/-}$/*Nrl*$^{-/-}$. Similarly, the fraction of the RPE occupied by lipofuscin granules was 4.9 fold higher in *Abca4*$^{-/-}$ than WT. The fraction of RPE occupied by lipofuscin granules in the *Abca4*$^{-/-}$/*Nrl*$^{-/-}$ was 2.8 fold higher than in the *Nrl*$^{-/-}$ but the difference did not achieve significance. In both the WT and *Nrl*$^{-/-}$ backgrounds, the average size of the lipofuscin granules was significantly larger in the absence of ABCA4 (Fig. 9C). Finally, we counted the number of phagocytosed OS pieces in the RPE. *Abca4*$^{-/-}$/*Nrl*$^{-/-}$ and *Nrl*$^{-/-}$ mice exhibit fewer pieces of OS in the RPE than their WT counterparts (Fig. 9D, 62% reduction in *Nrl*$^{-/-}$ compared to WT, and 54% reduction in *Abca4*$^{-/-}$/*Nrl*$^{-/-}$ compared to *Abca4*$^{-/-}$) although this reduction was not statistically significant. These data combined suggest that while A2E is generated at similar absolute levels in the WT and *Nrl*$^{-/-}$ background (and at higher levels in the *Nrl*$^{-/-}$ background when normalized to total 11-cisRAL), the amount of that A2E making it to the RPE is significantly less in the *Nrl*$^{-/-}$ background.

4. Discussion

Here we show that ABCA4 deficiency has a different effect in cones vs. rods. The main structural effect we observe in cone-dominant retinas lacking ABCA4 (*Abca4*$^{-/-}$/*Nrl*$^{-/-}$) is a significant reduction in rosette number compared to *Nrl*$^{-/-}$ retinas. We observe increased retinal stress as measured by GFAP in both rod- and cone- dominant retinas lacking ABCA4. Cones generate significantly more A2E per mole of retinoid than rods do, and as in the rod-dominant background, A2E accumulates abnormally in cone-dominant animals lacking ABCA4. However, fewer lipofuscin granules are detected in the RPE of cone-dominant ABCA4-deficient eyes than rod-dominant ABCA4-deficient eyes. Interestingly, the lighting conditions under which the animals were raised (30 lx vs. 300 lx) did not significantly exasperate the measured outcomes.

Since A2E formation initially results from abnormal accumulation of atRAL, it is not surprising that in dark reared *Abca4*$^{-/-}$ animals A2E accumulation was attenuated compared to animals raised under cyclic light at 30 lx [27]. Subsequent work demonstrated that A2E

levels were not significantly different in *Abca4*$^{-/-}$ animals reared under cyclic conditions at either 30, 120, or 1700 lx [28], although light exposure did stimulate formation of reactive forms of photooxidized A2E [13]. These results suggested that the adverse effects of light on A2E accumulation plateau at levels past 30 lx, i.e. that dark-rearing is protective compared to rearing at 30 lx but rearing at low light levels (30 lx) provides no benefits compared to rearing in brighter light (120 lx or 1700 lx). Rods contain the majority of 11-cisRAL in the WT murine retina with only a small cone contribution; thus it is possible that this plateauing effect is due to rod saturation which occurs at levels below 30 lx [29]. We hypothesized that in the cone-dominant background, light-dependent A2E accumulation might be more pronounced than in the rod-dominant background since cones are the major contributor of atRAL and they are actively undergoing phototransduction and thus retinoid cycling at both 30 and 300 lx [29]. However, we did not detect a significant effect of light exposure on accumulation of A2E or on any other structural or functional outcome. These data suggest two possibilities. The first is that the rate of cone retinoid cycling (and thus atRAL generation) is not more at 300 lx than it is at 30 lx, possibly due to light adaptation. Alternatively, under high light conditions, A2E production is actually increased, but that increase is not detected because high light levels also increase A2E photooxidation and photodegradation [9,28]. The simultaneous increase in A2E production and elimination by photooxidation and photodegradation would therefore lead to a lack of net change in overall A2E levels from low light to high light. In support of the latter possibility, we see a non-statistically significant reduction in A2E levels at P120 in *Abca4*$^{-/-}$/*Nrl*$^{-/-}$ mice reared at 300 lx compared to their counterparts reared at 30 lx. This light-associated decrease could reflect increased photooxidation and photodegradation of A2E.

Interestingly, we show that cones in the *Nrl*$^{-/-}$ have much higher rates of generation of A2E per mole of 11-cisRAL than rods do. These data are consistent with the differing properties of rod and cone phototransduction. First, under ambient lighting, cones are actively generating atRAL while rods are saturated. Second, cones have a much higher capacity for photoisomerization prior to saturation than rods (up to 1,000,000 vs. 500 photoisomerizations/s, respectively) and can recover sensitivity faster than rods [30–33]. These factors combined suggest that under light conditions, cones utilize more ret-inoid and place a significantly higher demand on the retinoid recycling system than rods do. It might not be surprising, therefore that abnormal accumulation of A2E in cones lacking ABCA4 (*Abca4*$^{-/-}$/*Nrl*$^{-/-}$) is much more pronounced than in rods lacking ABCA4 (*Abca4*$^{-/-}$ as in Fig. 8c). These data suggest that as a result of their higher levels of activity under ambient light, cones have a higher need for rapid and efficient clearance of atRAL and thus would be more sensitive than rods to interruptions in this clearance process (as would be the case in the absence of ABCA4). However, while the increased production of A2E per mole of 11-cisRAL in the *Nrl*$^{-/-}$ compared to WT is consistent with the physiology of cones vs. rods, we must also consider the potential effects of the degeneration inherent in the *Nrl*$^{-/-}$ model system (as evidenced by the decrease in ONL number in Fig. 3B). Evidence from the RCS rat which exhibits defects in OS phagocytosis and abnormal accumulation of A2E in photoreceptors prior to or concurrent with degeneration suggests that photoreceptor cells under stress may form accentuated levels of bis-retinoids as a result of aberrant handling of atRAL [34]. This phenomenon may contribute to the increased production of A2E in animals in the *Nrl*$^{-/-}$ background.

How then does increased cone accumulation of A2E relate to macular vision loss in Stargardt's patients? One of the distinguishing characteristics of the macula (which is modeled by the *Nrl*$^{-/-}$) is high cone density. In the peripheral retina, each RPE cell interacts with many rods but only a few cones. In contrast, in the macula, each RPE cell interacts with many cones. Under photopic conditions, when cones are the primary source of phototransduction and retinoid cycling, peripheral RPE cells would therefore only have to

accommodate the visual cycle for a couple of cells, in contrast to macular RPE cells which would support many photoreceptors. Thus in light these macular RPE would have much higher demands placed on them than non-macular RPE. RPE atrophy as a result of this demand coupled with ABCA4-related defects in retinoid processing has been thought to underlie macular vision loss in Stargardt's patients. Using the *Nrl*$^{-/-}$ mouse as a model for the macula, we here show that some cone-intrinsic toxicities may also contribute to macular vision loss. Our data indicate that the cone-dominant eye generates more A2E than the rod-dominant eye. Yet, in our morphometric analyses, we observe that significantly fewer (4.15 fold) lipofuscin granules are detected in the RPE of cone-dominant *Abca4*$^{-/-}$/*Nrl*$^{-/-}$ eyes than *Abca4*$^{-/-}$ eyes even though *Abca4*$^{-/-}$/*Nrl*$^{-/-}$ mice exhibit only 0.48 fold less A2E than *Abca4*$^{-/-}$. Thus A2E generated in cones may abnormally remain in or associated with the photoreceptor where it would be expected to exert its cytotoxic effects. These data suggest that macular vision loss is partly due to a direct toxic effect of accumulated A2E and/or its photooxidative products on cones rather than being entirely based on degeneration as a consequence of RPE atrophy. The anatomy of the cone OS supports this possibility. In rods, the discs are enclosed and self-contained, thus any A2PE/A2E generated therein would travel with the disc and eventually be phagocytosed by the RPE. In contrast, the cone lamellae membrane is contiguous with the plasma membrane; and membrane-associated-A2E and/or its photooxidative components may be found in other cellular compartments. These other cellular compartments, such as the inner segment, do not turn over membrane in the same way as OSs and therefore, A2E might be expected to accumulate in the cone cell rather than the RPE [35]. In a study examining cone OS shedding, Long et al. reported that lipofuscin-like particles were detected in cone ISs and Müller cell processes [36] in the cone-dominant ground squirrel retina. Similarly, Milam and colleagues reported Müller cell hypertrophy and accumulation of lipofuscin-like autofluorescence in the cone inner segments of the retina of a patient with Stargardt's disease [35]. These previous observations provide support for the hypothesis that A2E/lipofuscin may form not only in cone OS but also in cone ISs that do not undergo turnover.

A second (and related) explanation for accelerated macular vision loss in ABCA4-associated disease is that we detect several signs suggestive of a mild increase in cone degeneration (compared to rod) in the *Nrl*$^{-/-}$ retina in the absence of ABCA4. First, cone function is slightly decreased in *Abca4*$^{-/-}$/*Nrl*$^{-/-}$ at P120 compared to P30, while rod function has been demonstrated to be unaffected at this age [2]. Second, retinal stress as measured by GFAP induction was elevated in *Abca4*$^{-/-}$/*Nrl*$^{-/-}$ compared to *Abca4*$^{-/-}$. Third, although we did not detect any significant decreases in the number of cells in the ONL (Fig. 3), average ONL cell numbers for *Abca4*$^{-/-}$/*Nrl*$^{-/-}$ in the superior retina at P120 were consistently lower than those for *Nrl*$^{-/-}$ while averages in *Abca4*$^{-/-}$ were equivalent to *Abca4*$^{+/+}$. Fourth, we observe a reduction in rosette number in *Abca4*$^{-/-}$/*Nrl*$^{-/-}$ compared to *Nrl*$^{-/-}$, a phenotype associated with degeneration in other *Nrl*$^{-/-}$ models including the *rpe65*$^{-/-}$/*Nrl*$^{-/-}$ and the *rds*$^{-/-}$/*Nrl*$^{-/-}$ [24,25,37]. Finally, there are some data to suggest that cones may be more sensitive to oxidative stress than rods [38]. While these data suggest a slightly earlier onset of cone degeneration in the absence of *Abca4*$^{-/-}$ the effects are mild and the ongoing degeneration in the *Nrl*$^{-/-}$ itself must be remembered. In the WT background, significant ONL thinning is first detected at 8–9 months of age [23]. We see induction of GFAP in these mice at P120, consistent with GFAP induction as an early indicator of retinal stress. It is not clear why GFAP induction precedes ONL thinning by so substantial a margin, however a similar phenotype has been observed in models of cone dystrophy [39]. In the cpfl1 mouse model of cone dystrophy (Pde6c mutation), pan-retinal GFAP induction is associated with cone stress/degeneration and occurs prior to ONL thinning [39]. In the rod-dominant murine retina, ONL thinning primarily reflects rod photoreceptor death, and these observations suggest that cone stress/death can induce the type of GFAP induction we see in the *Abca4*$^{-/-}$ and *Abca4*$^{-/-}$/*Nrl*$^{-/-}$. It is striking that we did not observe more accelerated

degeneration in the *Abca4*$^{-/-}$/*Nrl*$^{-/-}$ mice. Abca4-associated Stargardt's is a juvenile-onset disease with central vision defects usually appearing in childhood or adolescence. Our observed lack of severe visual defects and severe degeneration from P30 to P120 indicates that the timecourse of disease development is different in humans and mice.

5. Conclusions

In conclusion, we here present evidence that cones and rods have an inherently different response to ABCA4 deficiency. Cones simultaneously generate more A2E and clear it less efficiently than rods, suggesting that primary A2E toxicity may play a role in the development of macular defects in cases of ABCA4 deficiency. These findings significantly enhance our understanding of the role of ABCA4 in rods and cones and have direct relevance to cone-based macular vision loss in patients afflicted with ABCA4-associated recessive Stargardt's.

Supplementary Material

Refer to Web version on PubMed Central for supplementary material.

Acknowledgments

Funding

This work was supported by grants from the National Institutes of Health [EY10609 (MIN), EY018656 (MIN), EY12951 (JRS) and EY018512 (SMC)], Core Grant for Vision Research EY12190, the Foundation Fighting Blindness (MIN).

The authors would like to thank Ms. Barb Nagel and Mr. Ryan Shaw for their technical assistance and Dr. Muayyad Al-Ubaidi for his comments on the manuscript.

Abbreviations

11-cisRAL	11-*cis*-retinaldehyde
ABCA4	retina-specific ATP binding cassette
atRAL	all-*trans*-retinaldehyde
GFAP	glial fibrillary acidic protein
INL	inner nuclear layer
IPL	inner plexiform layer
NRL	neural retina leucine zipper
ONL	outer nuclear layer
OS	outer segment
P	post-natal day
RDS	retinal degeneration slow
ROM1	rod outer segment membrane protein 1
RPE	retinal pigment epithelium
WT	wild-type

References

1. Sun H, Nathans J. Stargardt's ABCR is localized to the disc membrane of retinal rod outer segments. Nat Genet. 1997; 17:15–16. [PubMed: 9288089]
2. Weng J, Mata NL, Azarian SM, Tzekov RT, Birch DG, Travis GH. Insights into the function of Rim protein in photoreceptors and etiology of Stargardt's disease from the phenotype in abcr knockout mice. Cell. 1999; 98:13–23. [PubMed: 10412977]
3. Illing M, Molday LL, Molday RS. The 220-kDa rim protein of retinal rod outer segments is a member of the ABC transporter superfamily. J Biol Chem. 1997; 272:10303–10310. [PubMed: 9092582]
4. Molday RS. ATP-binding cassette transporter ABCA4: molecular properties and role in vision and macular degeneration. J Bioenerg Biomembr. 2007; 39:507–517. [PubMed: 17994272]
5. Molday LL, Rabin AR, Molday RS. ABCR expression in foveal cone photoreceptors and its role in Stargardt macular dystrophy. Nat Genet. 2000; 25:257–258. [PubMed: 10888868]
6. Sullivan JM. Focus on molecules: ABCA4 (ABCR)—an import-directed photoreceptor retinoid flipase. Exp Eye Res. 2009; 89:602–603. [PubMed: 19306869]
7. Sun H, Nathans J. Mechanistic studies of ABCR, the ABC transporter in photoreceptor outer segments responsible for autosomal recessive Stargardt disease. J Bioenerg Biomembr. 2001; 33:523–530. [PubMed: 11804194]
8. Hoffman CJ, Miller RH, Hultin MB. Correlation of factor VII activity and antigen with cholesterol and triglycerides in healthy young adults. Arterioscler Thromb. 1992; 12:267–270. [PubMed: 1547186]
9. Wu Y, Yanase E, Feng X, Siegel MM, Sparrow JR. Structural characterization of bisretinoid A2E photocleavage products and implications for age-related macular degeneration. Proc Natl Acad Sci U S A. 2010; 107:7275–7280. [PubMed: 20368460]
10. Parish CA, Hashimoto M, Nakanishi K, Dillon J, Sparrow J. Isolation and one-step preparation of A2E and iso-A2E, fluorophores from human retinal pigment epithelium. Proc Natl Acad Sci U S A. 1998; 95:14609–14613. [PubMed: 9843937]
11. Sparrow JR, Parish CA, Hashimoto M, Nakanishi K. A2E, a lipofuscin fluorophore, in human retinal pigmented epithelial cells in culture. Investig Ophthalmol Vis Sci. 1999; 40:2988–2995. [PubMed: 10549662]
12. De S, Sakmar TP. Interaction of A2E with model membranes. Implications to the pathogenesis of age-related macular degeneration. J Gen Physiol. 2002; 120:147–157. [PubMed: 12149277]
13. Ben-Shabat S, Itagaki Y, Jockusch S, Sparrow JR, Turro NJ, Nakanishi K. Formation of a nonaoxirane from A2E, a lipofuscin fluorophore related to macular degeneration, and evidence of singlet oxygen involvement. Angew Chem Int Ed Engl. 2002; 41:814–817. [PubMed: 12491345]
14. Rozanowska M, Jarvis-Evans J, Korytowski W, Boulton ME, Burke JM, Sarna T. Blue light-induced reactivity of retinal age pigment. In vitro generation of oxygen-reactive species. J Biol Chem. 1995; 270:18825–18830. [PubMed: 7642534]
15. Zhou J, Kim SR, Westlund BS, Sparrow JR. Complement activation by bisretinoid constituents of RPE lipofuscin. Investig Ophthalmol Vis Sci. 2009; 50:1392–1399. [PubMed: 19029031]
16. Pawar AS, Qtaishat NM, Little DM, Pepperberg DR. Recovery of rod photoresponses in ABCR-deficient mice. Investig Ophthalmol Vis Sci. 2008; 49:2743–2755. [PubMed: 18263807]
17. Daniele LL, Lillo C, Lyubarsky AL, Nikonov SS, Philp N, Mears AJ, Swaroop A, Williams DS, Pugh EN Jr. Cone-like morphological, molecular, and electrophysiological features of the photoreceptors of the Nrl knockout mouse. Invest Ophthalmol Vis Sci. 2005; 46:2156–2167. [PubMed: 15914637]
18. Mears AJ, Kondo M, Swain PK, Takada Y, Bush RA, Saunders TL, Sieving PA, Swaroop A. Nrl is required for rod photoreceptor development. Nat Genet. 2001; 29:447–452. [PubMed: 11694879]
19. Tan E, Wang Q, Quiambao AB, Xu X, Qtaishat NM, Peachey NS, Lem J, Fliesler SJ, Pepperberg DR, Naash MI, Al-Ubaidi MR. The relationship between opsin overexpression and photoreceptor degeneration. Investig Ophthalmol Vis Sci. 2001; 42:589–600. [PubMed: 11222515]

20. Ding XQ, Nour M, Ritter LM, Goldberg AF, Fliesler SJ, Naash MI. The R172W mutation in peripherin/rds causes a cone-rod dystrophy in transgenic mice. Hum Mol Genet. 2004; 13:2075–2087. [PubMed: 15254014]
21. Chakraborty D, Conley SM, Stuck MW, Naash MI. Differences in RDS traffick-ing, assembly and function in cones versus rods: insights from studies of C150S-RDS. Hum Mol Genet. 2010; 19:4799–4812. [PubMed: 20858597]
22. Kim SR, Jang YP, Sparrow JR. Photooxidation of RPE lipofuscin bisretinoids enhances fluorescence intensity. Vision Res. 2010; 50:729–736. [PubMed: 19800359]
23. Wu L, Nagasaki T, Sparrow JR. Photoreceptor cell degeneration in abcr (−/−) mice. Adv Exp Med Biol. 2010; 664:533–539. [PubMed: 20238056]
24. Farjo R, Fliesler SJ, Naash MI. Effect of Rds abundance on cone outer segment morphogenesis, photoreceptor gene expression, and outer limiting membrane integrity. J Comp Neurol. 2007; 504:619–630. [PubMed: 17722028]
25. Farjo R, Skaggs JS, Nagel BA, Quiambao AB, Nash ZA, Fliesler SJ, Naash MI. Retention of function without normal disc morphogenesis occurs in cone but not rod photoreceptors. J Cell Biol. 2006; 173:59–68. [PubMed: 16585269]
26. Feathers KL, Lyubarsky AL, Khan NW, Teofilo K, Swaroop A, Williams DS, Pugh EN Jr, Thompson DA. Nrl-knockout mice deficient in Rpe65 fail to synthesize 11-cis retinal and cone outer segments. Investig Ophthalmol Vis Sci. 2008; 49:1126–1135. [PubMed: 18326740]
27. Mata NL, Weng J, Travis GH. Biosynthesis of a major lipofuscin fluorophore in mice and humans with ABCR-mediated retinal and macular degeneration. Proc Natl Acad Sci U S A. 2000; 97:7154–7159. [PubMed: 10852960]
28. Radu RA, Mata NL, Bagla A, Travis GH. Light exposure stimulates formation of A2E oxiranes in a mouse model of Stargardt's macular degeneration. Proc Natl Acad Sci U S A. 2004; 101:5928–5933. [PubMed: 15067110]
29. Umino Y, Solessio E, Barlow RB. Speed, spatial, and temporal tuning of rod and cone vision in mouse. J Neurosci. 2008; 28:189–198. [PubMed: 18171936]
30. Baylor DA, Lamb TD, Yau KW. The membrane current of single rod outer segments. J Physiol. 1979; 288:589–611. [PubMed: 112242]
31. Perry RJ, McNaughton PA. Response properties of cones from the retina of the tiger salamander. J Physiol. 1991; 433:561–587. [PubMed: 1841958]
32. Baylor DA, Nunn BJ, Schnapf JL. The photocurrent, noise and spectral sensitivity of rods of the monkey Macaca fascicularis. J Physiol. 1984; 357:575–607. [PubMed: 6512705]
33. Schnapf JL, Nunn BJ, Meister M, Baylor DA. Visual transduction in cones of the monkey Macaca-fascicularis. J Physiol (Lond). 1990; 427:681–713. [PubMed: 2100987]
34. Sparrow JR, Yoon KD, Wu Y, Yamamoto K. Interpretations of fundus autofluorescence from studies of the bisretinoids of the retina. Investig Ophthalmol Vis Sci. 2010; 51:4351–4357. [PubMed: 20805567]
35. Birnbach CD, Jarvelainen M, Possin DE, Milam AH. Histopathology and immunocytochemistry of the neurosensory retina in fundus flavimaculatus. Ophthalmology. 1994; 101:1211–1219. [PubMed: 8035984]
36. Long KO, Fisher SK, Fariss RN, Anderson DH. Disc shedding and autophagy in the cone-dominant ground squirrel retina. Exp Eye Res. 1986; 43:193–205. [PubMed: 3758219]
37. Kunchithapautham K, Coughlin B, Crouch RK, Rohrer B. Cone outer segment morphology and cone function in the $Rpe65^{-/-}$ $Nrl^{-/-}$ mouse retina are amenable to retinoid replacement. Invest Ophthalmol Vis Sci. 2009; 50:4858–4864. [PubMed: 19407011]
38. Rogers BS, Symons RC, Komeima K, Shen J, Xiao W, Swaim ME, Gong YY, Kachi S, Campochiaro PA. Differential sensitivity of cones to iron-mediated oxidative damage. Investig Ophthalmol Vis Sci. 2007; 48:438–445. [PubMed: 17197565]
39. Schaeferhoff K, Michalakis S, Tanimoto N, Fischer MD, Becirovic E, Beck SC, Huber G, Rieger N, Riess O, Wissinger B, Biel M, Seeliger MW, Bonin M. Induction of STAT3-related genes in fast degenerating cone photoreceptors of cpfl1 mice. Cell Mol Life Sci. 2010; 67:3173–3186. [PubMed: 20467778]

Appendix A. Supplementary data

Supplementary data to this article can be found online at doi:10. 1016/j.bbadis.2011.10.007.

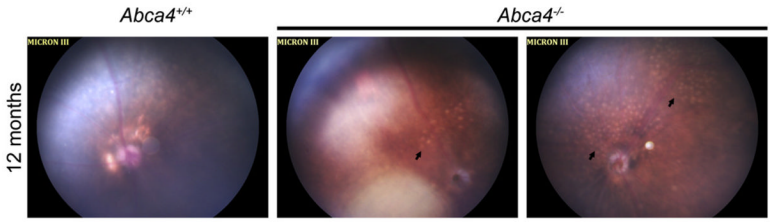

Fig. 1.

Development of retinal flecking and atrophic areas in the *Abca4*$^{-/-}$ mouse. Fundus images were collected from anesthetized mice at the age of 12 months. On the left is shown a normal aged fundus (*Abca4*$^{+/+}$), on the middle and right are shown two representative images collected from age-matched *Abca4*$^{-/-}$ mice. Note the appearance of yellowish flecks and atrophic areas (arrows).

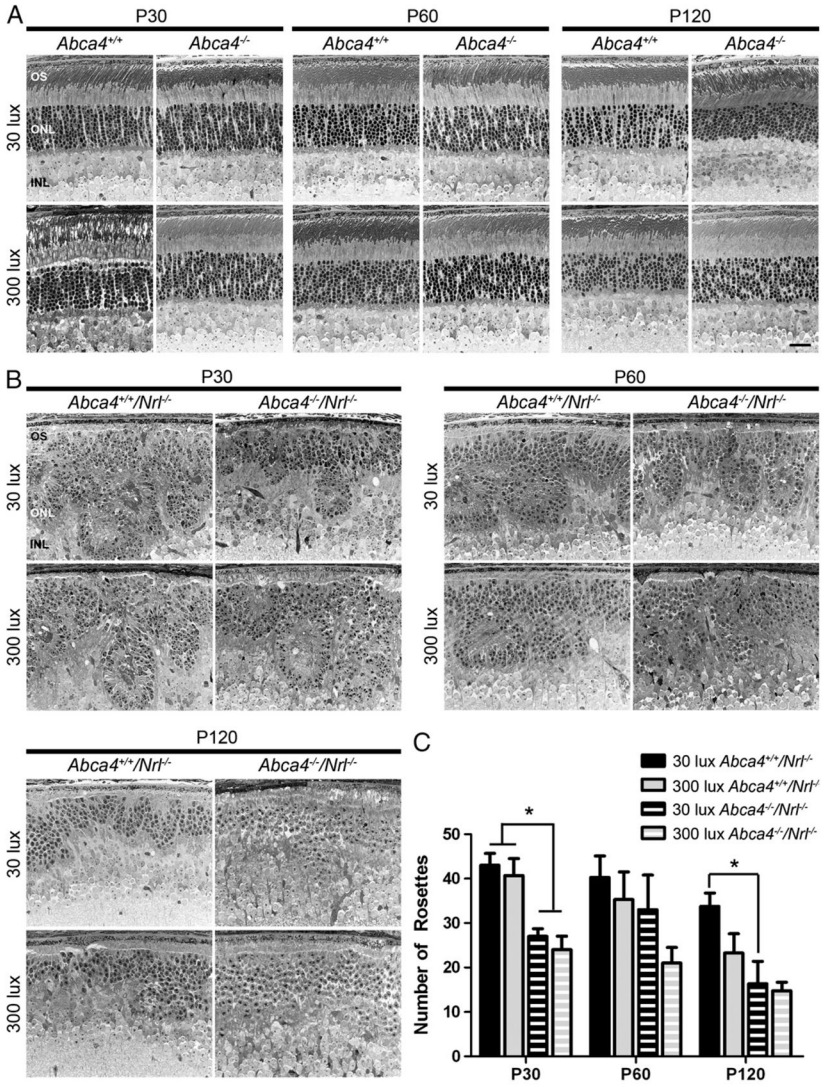

Fig. 2.

Structural effects of ABCA4 deficiency. Representative sections from *Abca4*$^{+/+}$ and *Abca4*$^{-/-}$(A), *Abca4*$^{+/+}$/*Nrl*$^{-/-}$ and *Abca4*$^{-/-}$/*Nrl*$^{-/-}$(B) reared at 30 (top rows) or 300 lx (bottom rows) were collected at P30, P60 and P120. (A) No overt changes in retinal structure are observed in the absence of ABCA4 in the WT background. (B) In the *Nrl*$^{-/-}$ background, the primary structural defect arising from ABCA4 deficiency is a decrease in the number rosettes detected in the outer nuclear layer (ONL). Light rearing had no discernible effect on any genotype. (C) Rosettes were quantified in central retinal sections in 3–5 mice per group. Values are presented as mean total rosettes counted±SEM. * $p<0.05$. OS: outer segment, ONL: outer nuclear layer, INL: inner nuclear layer. Scale bar 25 μm.

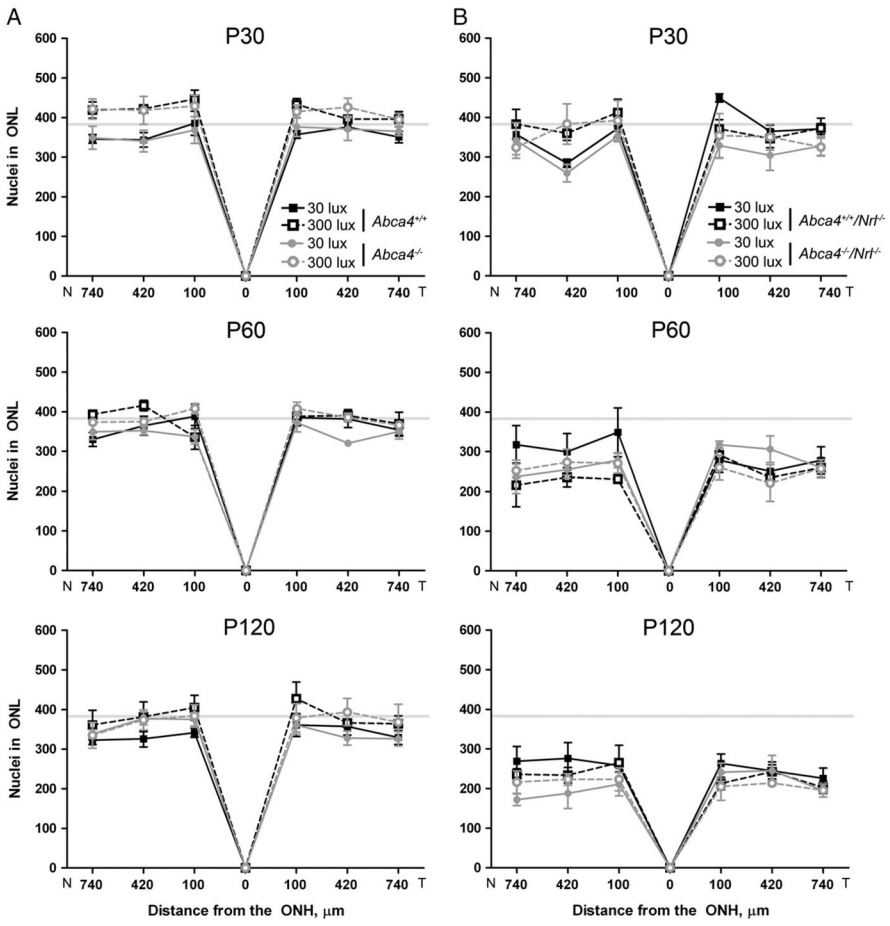

Fig. 3.

ABCA4 deficiency does not increase retinal degeneration up to P120. Measuring from the optic nerve head, sections (as in Fig. 2) were imaged at 100 μm intervals. Total nuclei in the ONL were counted in each image from 3 to 5 mice per group. Values are presented as mean ±SEM. Horizontal gray lines represent average levels at P30. (A) WT mice and their ABCA4 deficient counterparts do not exhibit any retinal thinning up to P120 at either light level. (B) In the $Nrl^{-/-}$ background, a decrease in ONL thickness is observed by P120 but neither lack of ABCA4 nor light exposure has any significant effect on the decrease. N: nasal, T: temporal.

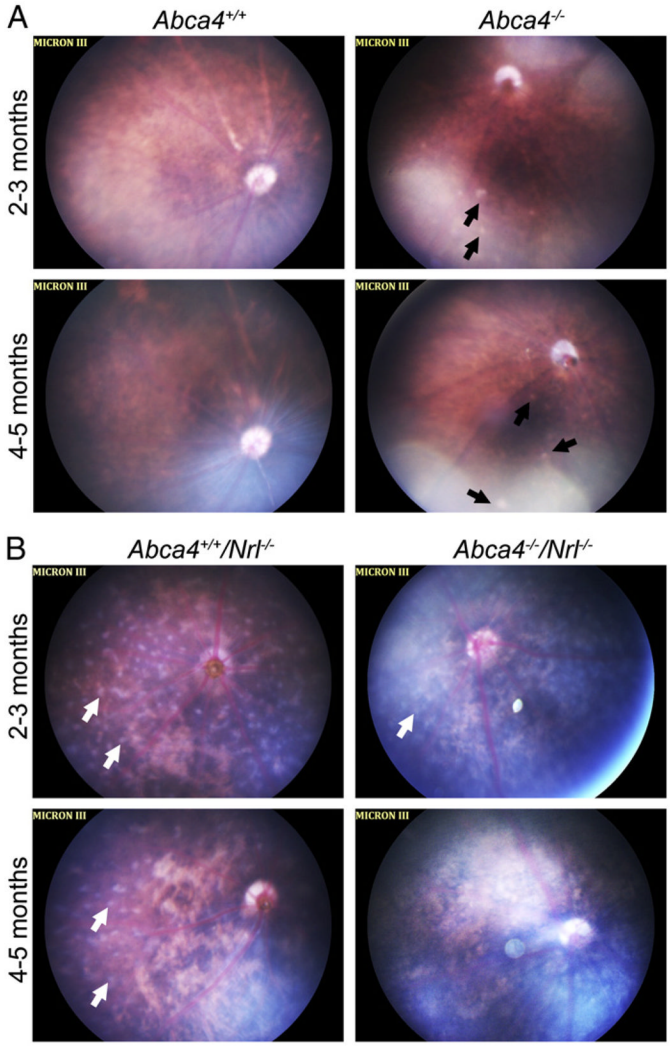

Fig. 4.

Development of retinal flecking in the absence of ABCA4. Shown are representative fundus images captured from animals raised at 30 lx at 2–3 months of age (top row of each panel) or 4–5 months of age (bottom row of each panel) in the WT (A) or *Nrl*$^{-/-}$(B) background. (A) Normal fundus (left) and *Abca4*$^{-/-}$ fundus (right). At both ages, some *Abca4*$^{-/-}$ animals exhibited signs of retinal flecking (black arrows) while others exhibited a normal fundus. (B) *Abca4*$^{+/+}$/*Nrl*$^{-/-}$ fundus (left) and *Abca4*$^{-/-}$/*Nrl*$^{-/-}$ fundus (right). The *Nrl*$^{-/-}$ fundus at 2–3 months of age exhibits evenly spaced white-gray spots across the fundus (white arrows). By 4–5 months of age these spots are detected primarily in the periphery with very few in the central portion. In the *Abca4*$^{-/-}$/*Nrl*$^{-/-}$ eye, the white-gray spots are detected at 2–3 months, although not to the same extent as in the *Abca4*$^{+/+}$/*Nrl*$^{-/-}$. Very few white-gray spots are detected in *Abca4*$^{-/-}$/*Nrl*$^{-/-}$ eyes at 4–5 months. No signs of retinal flecking are observed in the *Nrl*$^{-/-}$ background at either age.

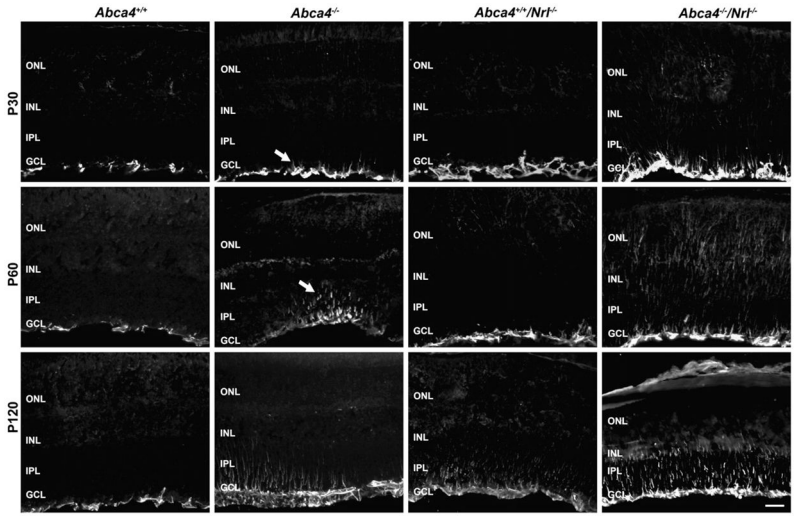

Fig. 5.

Retinal stress is exacerbated in the absence of ABCA4. Frozen retinal sections collected at P30, 60, and 120 were stained with the retinal stress marker, GFAP. At P30 (top) and P60 (middle) normal GFAP localization is observed in *Abca4*$^{+/+}$ and *Abca4*$^{+/+}$/*Nrl*$^{-/-}$ retinas, expression is limited to the inner limiting membrane. Very mild GFAP induction is observed at P30 age in *Abca4*$^{-/-}$ and *Abca4*$^{-/-}$/*Nrl*$^{-/-}$ animals (arrowheads). At P60 patchy induction of GFAP is seen in *Abca4*$^{-/-}$ animals (arrows) and induction is seen throughout *Abca4*$^{-/-}$/*Nrl*$^{-/-}$ retinas. By P120, all genotypes except *Abca4*$^{+/+}$ show signs of GFAP induction, with the most severe being detected in the *Abca4*$^{-/-}$/*Nrl*$^{-/-}$. Scale bar 25 μm. ONL: outer nuclear layer, INL: inner nuclear layer, IPL: inner plexiform layer, GCL: ganglion cell layer.

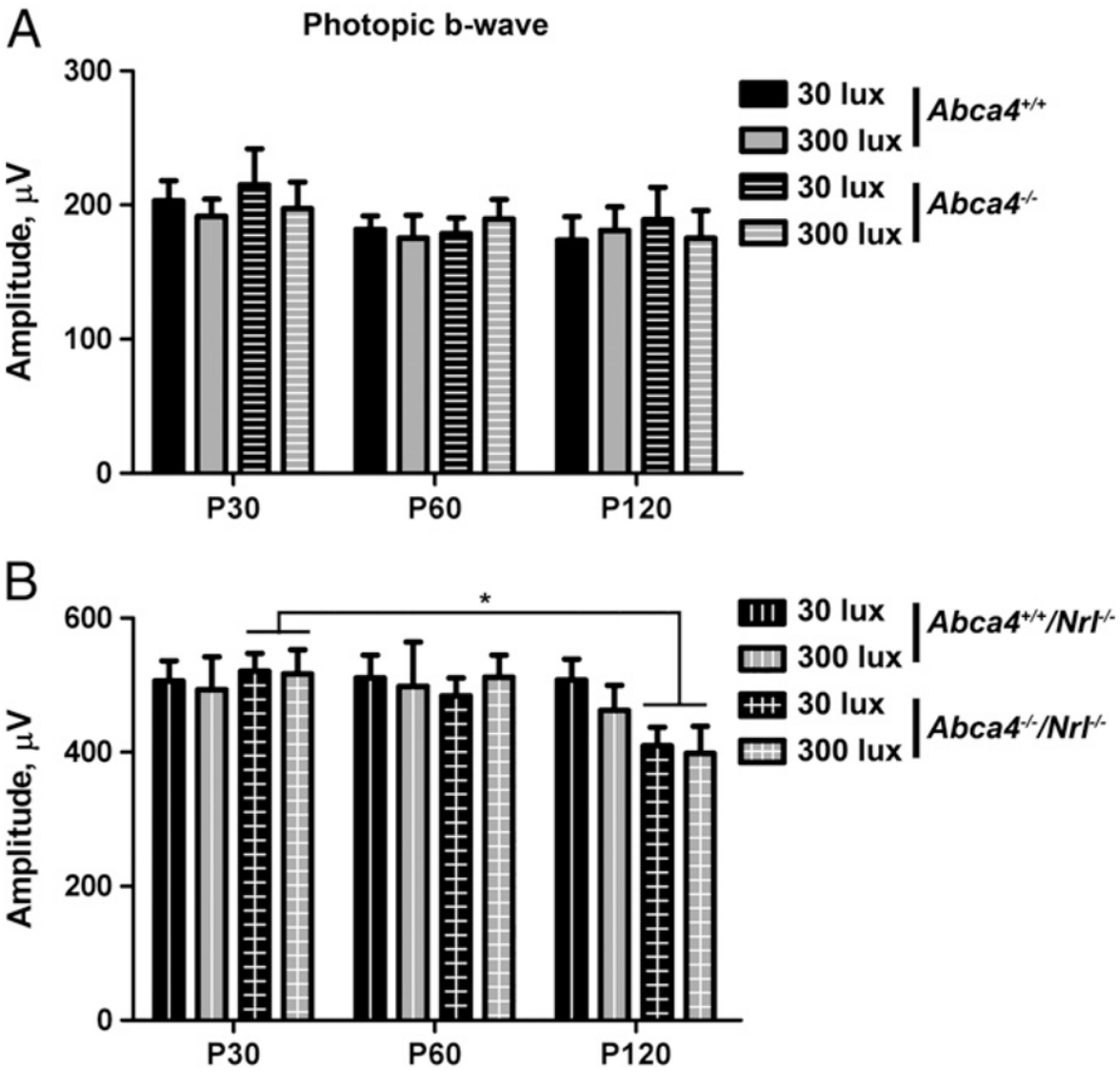

Fig. 6.

Cone function is not severely affected by ABCA4 deficiency. Full-field scotopic ERGs were performed on 6–8 animals per group at P30, 60, and 120. Results shown are mean maximum amplitudes±SEM. (A) In the WT background, ABCA4 deficiency has no effect on cone function. (B) In the $Nrl^{-/-}$ background, a mild decrease in cone function is observed in $Abca4^{-/-}/Nrl^{-/-}$ animals at P120 compared to P30. * $p<0.05$.

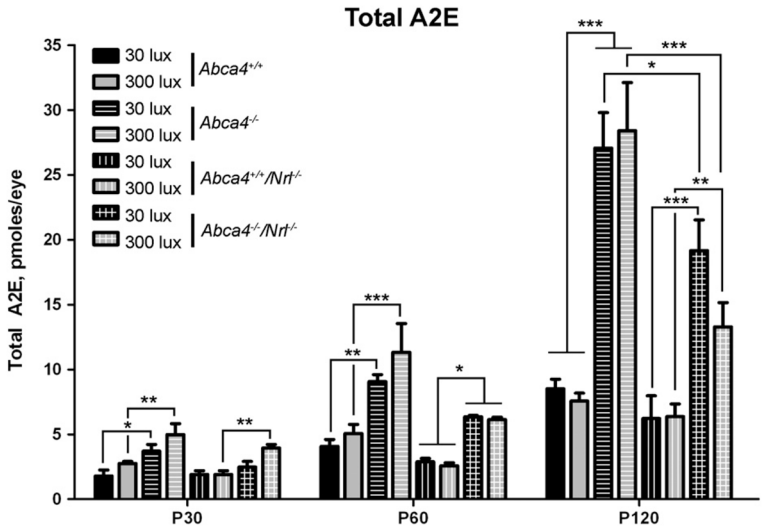

Fig. 7.

A2E levels are significantly increased in the absence of ABCA4. Total A2E levels were measured from eyecups harvested at P30, 60 or 120. 3–6 independent samples were measured for each group and values are presented as mean pmoles of A2E/eye±SEM. Rearing under 300 lx did not have a significant effect on A2E accumulation but at every timepoint, in both the WT and *Nrl*$^{-/-}$ background, animals lacking ABCA4 accumulated significantly more A2E than control animals. *p<0.05, **p<0.01, ***p<0.001.

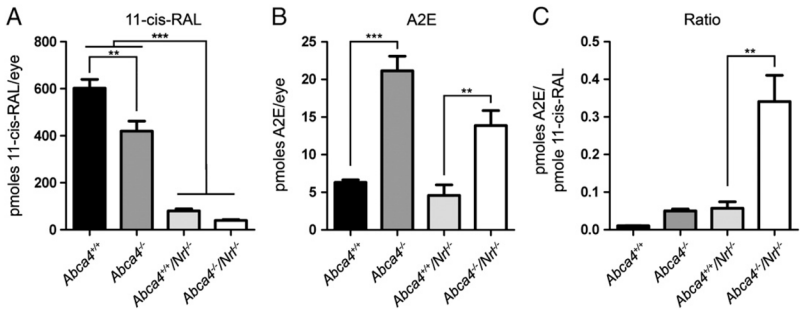

Fig. 8.

11-cisRAL levels are decreased in the absence of ABCA4. 11-cisRAL levels were measured from eyecups harvested at P120 (30 lx), 4–5 measurements per group. (a) 11-cisRAL levels are significantly decreased in the *Nrl*$^{-/-}$ background. (b) For clarity's sake, A2E values at P120 (30 lx) from Fig. 8 are shown here. (c) A2E values are shown normalized to 11-cisRAL levels. Per pmole of 11-cisRAL, animals in the *Nrl*$^{-/-}$ background, particularly when lacking ABCA4, accumulate significantly more A2E than animals in the WT background. *p<0.05, **p<0.01, ***p<0.001.

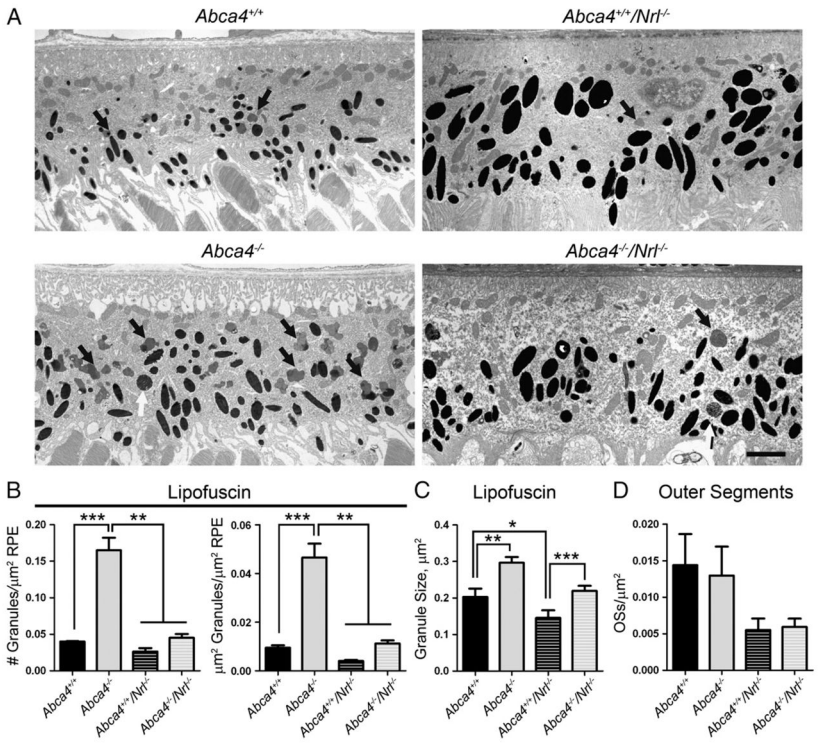

Fig. 9.

Fewer lipofuscin granules are detected in the RPE cells of ABCA4 deficient eyes in the *Nrl*$^{-/-}$ background when compared to the WT background. (A) Representative electron micrographs of the RPE cell layer at P120 showing lipofuscin granules (black arrows) and phagocytosed outer segments (white arrows). Scale bar 2 μm. For quantification, 3–5 animals per group were analyzed and at least 5 images per eye were counted, totals were summed for each eye and values shown are means±SEM. (B) Both the number of lipofuscin granules per μm of RPE area (left) and the fraction of RPE occupied by lipofuscin granules (right) are increased with significance in the *Abca4*$^{-/-}$ compared to all other genotypes, and these parameters are also non-significantly increased in *Abca4*$^{-/-}$/*Nrl*$^{-/-}$ compared to *Abca4*$^{+/+}$/*Nrl*$^{-/-}$. (C) In both the WT and *Nrl*$^{-/-}$ backgrounds, the average size of each lipofuscin granule is larger in the absence of ABCA4. (D) In the *Nrl*$^{-/-}$ background the number of OS pieces detected inside the RPE appeared to be less than in the WT background, but the difference was not statistically significant. *p<0.05, **p<0.01, ***p<0.001.